Environmental Science Processes & Impacts

PAPER

View Article Online
View Journal | View Issue

Cite this: *Environ. Sci.: Processes Impacts*, 2016, **18**, 1011

Phospholipophilicity of $C_xH_yN^+$ amines: chromatographic descriptors and molecular simulations for understanding partitioning into membranes†

S. T. J. Droge,*[a] J. L. M. Hermens,[a] J. Rabone,[b] S. Gutsell[b] and G. Hodges[b]

Received 26th February 2016
Accepted 14th April 2016

DOI: 10.1039/c6em00118a

rsc.li/process-impacts

Using immobilized artificial membrane high-performance liquid chromatography (IAM-HPLC) the sorption affinity of 70 charged amine structures to phospholipids was determined. The amines contained only 1 charged moiety and no other polar groups, the rest of the molecule being aliphatic and/or aromatic hydrocarbon groups. We systematically evaluated the influence of the amine type (1°, 2°, 3° amines and quaternary ammonium), alkyl chain branching, phenyl ring positioning, charge positioning (terminal *vs.* central in the molecule) on the phospholipid-water partitioning coefficient (K_{PLIPW}). These experimental results were compared with quantum-chemistry based three-dimensional (3D) molecular simulations of the partitioning of charged amines, including the most likely solute conformers, using a hydrated phospholipid bilayer in the COSMOmic module of COSMOtherm software. Both IAM-HPLC retention data and the simulations suggest that the molecular orientation of charged amines at the location in the bilayer with the lowest calculated Gibbs free energy exerts a strong influence over the partitioning within the membrane. The most favourable position of charged amines coincides with the region where the phosphate anions in the phospholipid bilayer are most abundant. Hydrocarbon units oriented in this layer are located more towards the aqueous phase and contribute less to the overall membrane affinity than hydrocarbon units extending into the more hydrophobic core of the bilayer. COSMOmic simulations explain most of the trends between the structural differences observed in IAM-HPLC based K_{PLIPW}. For this set of cationic structures, the mean absolute difference between COSMOmic simulations and IAM-HPLC data, accounting only for amine type corrective increments, is 0.31 log units.

Environmental impact

Ionisable organic compounds pose a great challenge to accurate environmental fate/risk modelling, because most models have been designed to deal with neutral compounds only. The role of ionic species in partitioning to environmental phases can be substantial, particularly for quaternary ammonium compounds, but predictive models are lacking because of data scarcity. This study presents the largest consistent set of measurements on the partitioning affinity of simple cationic organic chemicals to a monolayer of phospholipids. In combination with quantum chemistry based molecular simulations, this study reveals that the sorption affinity depends on the orientation of cationic molecules in an anisotropic membrane structure, and that the simulated affinities can be used in accurate predictive models for membrane partitioning.

1. Introduction

Information about cell membrane partitioning is relevant in pharmaceutical, toxicological and environmental research. The membrane partition coefficient is a widely applied parameter in exposure, transport and kinetic modeling in both drug design and toxicology.[1] For ionizable compounds in particular, such a partition coefficient provides significant potential advantages over traditional measures of hydrophobicity such as the octanol–water partition coefficient (log *P*), for understanding partitioning processes important for bioaccumulation beyond those considering neutral lipids.[2] Several experimental techniques are available to measure or estimate membrane partitioning, including liposome suspensions, solid supported membranes, and HPLC columns.[3–8] Also, computational models have been developed to predict membrane partitioning.[9–11] Models are well developed for the prediction of partitioning of neutral compounds into membranes,[10] usually based on the octanol–water partition coefficients (log *P*) or linear free energy

[a]*Institute for Risk Assessment Sciences, Utrecht University, Yalelaan 104, 3508 TD Utrecht, The Netherlands. E-mail: steven.droge@gmail.com; Tel: +31 30 2535217*
[b]*Safety and Environmental Assurance Centre, Unilever, Sharnbrook, Bedford, UK*

† Electronic supplementary information (ESI) available: Chemical properties and simulation data in Tables S1 and S2, ESI-Fig. S1–S12. See DOI: 10.1039/c6em00118a

relationships (LFERs) using the more basic solute descriptors of molecular volume, polarizability and hydrogen bond forming capacities.[10,12,13] However, the predictions become highly uncertain for ionized organic compounds (IOCs) because of the lack of adequate models and molecular descriptors.[6] The major challenges in understanding the influence of molecular descriptors on the membrane binding affinity of charged IOCs is dealing with the anisotropic and (zwitter)ionic character of phospholipid membranes, and deriving meaningful descriptors for ionic sorbates (which may strongly differ from corresponding neutral species). There is a definitive need for reliable computational models to predict sorption affinities with phospholipid membranes (K_{PLIPW}), as well as other sorption processes in, for example, environmental and toxicological pathway research. Many of the existing chemicals that have to be assessed for their potential risk to human health and ecosystems are ionic compounds.[14] Recent reviews on the K_{PLIPW} of IOCs retrieved data for only 36 organic bases and 56 organic acids.[2,11,15]

COSMOmic (*i.e.*, COSMO-RS for micelles, based on the conductor like Screening Model for Real Solvents used in the software COSMOtherm) has recently been shown to be an efficient computational method for simulating the free energy of organic ions in their most favourable positioning and orientation in a hydrated phospholipid bilayer.[11,15] The set of K_{PLIPW} values for the 92 IOCs was predicted with a root-mean-square error (RMSE) of 0.7 log units by molecular simulations with COSMOmic, after fitting a positive internal membrane dipole potential. However, the structural diversity in that set of compounds does not readily allow for a systematic evaluation of the influence of specific molecular features on the partition behaviour of IOCs into membranes.

Immobilized artificial membrane high-performance liquid chromatography (IAM-HPLC) was used to generate a consistent set of accurate experimental K_{PLIPW} values for organic cations, in a relatively high-throughput standardised way compared to liposomal partitioning studies.[16] The IAM-HPLC column is packed with porous silica particles covered with a monolayer coating of covalently linked dialkyl-phospholipids, and retention on these particles can be directly related to the sorption affinity of the solutes. Our previous data set comprised 14 organic cations including archetypical amines and several basic pharmaceuticals and showed close overlap between IAM-HPLC results and liposomal partitioning data.[16] The current study will provide a first evaluation of IAM-HPLC measurements and COSMOmic simulations on an extensive series of simple organic cation structures, containing only hydrocarbon units and one charged nitrogen (molecular formula $C_xH_yN^+$), thus lacking any other polar moieties. Another set of optimized IAM-HPLC measurements on charged amines with a range of polar moieties will be published elsewhere. Although liposomal partitioning data have been compiled for up to 36 organic cations,[15] the current study fully focuses on a comparison between IAM-HPLC based data and COSMOmic predictions, (i) to ensure of a comparison based on only highly consistent experimental data (IAM-HPLC column used under optimized eluent conditions), (ii) to evaluate the membrane sorption process for a much wider range of chemical structures than the liposomal data set, (iii) to avoid mixing IAM-HPLC results with liposomal partitioning data, because despite the close overlap for 14 organic cations mentioned above[16] it remains to be evaluated to what extent sorption to the monolayer phospholipid coating in IAM-HPLC is representative for partitioning of organic cations into membrane bilayers, as present in dissolved liposomes and as modeled by COSMOmic. Differences in experimental findings between simple molecular structures should provide direct information on the influence that the different types of hydrocarbon units have on the partitioning to phospholipid membrane, for example those attached to the charged amine, or part of linear alkyl chains, branched groups, (aromatic) rings, and also on how the charged amine is positioned within the simple molecular structure. Combining experimental data and quantum chemical simulations, this study should also provide insights into the importance of the energetically most favourable orientation of ionic molecules sorbed in a phospholipid membrane. The consistent IAM-HPLC based experimental data on wide ranging series of amines may additionally serve as a validation set for predictions by the COSMOmic molecular simulations. Studying only $C_xH_yN^+$ structures allows for a systematic check on the basic trends for series of analogues in either IAM-HPLC data or COSMOmic simulations, as it will be more clear why predictions deviate more from observations for some compounds compared to others, which is much more difficult if IOCs with many types of polar groups and higher structural complexity (*e.g.* internal hydrogen bonding) are included. The data set will finally be used to model the K_{PLIPW} for $C_xH_yN^+$ structures as a single chemical domain, which could be a starting point for models for a broader chemical domain of organic cations.

2. Materials and methods

2.1 Test compounds

Seventy $C_xH_yN^+$ amines, listed in Table 1, were purchased as free base or salt from various suppliers (ESI Table S1†). All contained only a single amine and hydrocarbon moieties, with the exception of imipramine (amine #55), which has a second (nonionizable) nitrogen (structures in ESI-Fig. S1†). All compounds had a purity of >97%, and stock solutions were prepared as ~10 mg in 1 mL methanol (Biosolve BV, Valkenswaard, NL).

2.2 IAM column and eluents

A 10 cm × 4.6 mm IAM.PC.DD2 column (Regis Technologies, Inc., Morton Grove, IL USA) was used with an IAM.PC.DD2 10/300 guard cartridge in front. A flow rate of 1.0 mL min^{-1} was used throughout this study, with the column maintained at room temperature (23 ± 2 °C). Methanol stock solutions of the test chemicals were diluted >100 times in the applied eluent, and 20 μL was injected. The aqueous eluent used for UV-diode array detection consisted of 10 mM buffer (ammonium acetate/acetic acid for pH 5.0, phosphoric acid for pH 3.0), with an additional 8.0 g L^{-1} NaCl (137 mM) and 0.2 g L^{-1} KCl (2.7 mM),

Table 1 Experimental affinities for IAM-HPLC (K_{IAM} pH 5 ~ $K_{PLIPW} = 18.9 \times k_{IAM}$), simulated affinities (K_{DMPC}) and chemical properties (pK_a and log P) of $C_xH_yN^+$ amines (continues on next page)

				log K_{IAM} pH 3.0			log K_{IAM} pH 5.0			ΔpH_{5-3}[c]	log K_{PLIPW}	log K_{DMPC}	log P[e]
Amine type	#	Chemical name	pK_a[a]	*50*	Diff[b]	*N*	*46*	Diff[b]	*N*	*26*	Cation	Cation	Neutral
1°	1	Benzylamine	9.3	0.85	0.05	3	0.93	0.00	3	0.07	0.93	1.49	1.1
	2	4-Methylbenzylamine	9.4	1.31	0.04	2	1.40	0.00	3	0.09	1.40	1.96	1.6
	3	4-Butylbenzylamine	***9.5***	2.69		1					2.80	3.49	3.1
	4	4-Octylbenzylamine	***9.5***	4.84		4					4.96	5.89	5.3
	5	2-Phenylethylamine	9.8	1.42	0.05	2	1.51	0.00	3	0.09	1.51	1.89	1.5
	6	Amphetamine	10.1	1.19	0.05	3	1.27	0.00	3	0.07	1.27	1.84	1.8
	7	3-Phenylpropylamine	10.2	1.55	0.05	2	1.63	0.00	3	0.08	1.63	2.20	1.8
	8	4-Phenylbutylamine	10.4	1.90	0.05	2	1.98	0.00	3	0.08	1.98	2.65	2.4
	9	4-*t*-Butylcyclohexylamine	***10.5***				2.3/2.4[d]				2.29	2.73	3.1
	10	1-Hexylamine	10.6				1.32	0.01	3		1.32	2.26	2.0
	11	1-Heptylamine	10.7				1.74		1		1.74	2.80	2.5
	12	1-Octylamine	10.7				2.30		1		2.30	3.36	3.1
	13	1-Decylamine	10.6				3.60				3.60	4.48	4.1
	14	*tert*-Octylamine	***10.7***				1.49	0.00	3		1.49	1.64	2.3
	15	(±)-1-Aminoindane	9.2	1.31	0.05	2	1.40	0.00	3	0.09	1.40	1.59	1.6
	16	Amantadine	***10.7***				1.64		1		1.64	1.61	2.3
	17	1-Naphthylmethylamine	***9.7***	2.06	0.03	2	2.13	0.00	3	0.07	2.13	2.27	2.2
	18	1-Naphthylamine	3.9	2.09		1					2.21	1.94	2.2
	19	3,4-Dimethylaniline	5.2	1.55	0.00	3					1.55	2.07	1.9
	20	2,4,6-Trimethylaniline	4.4	1.86	0.01	3					1.86	1.76	2.3
	21	4-Octylaniline	***4.8***	5.11		2					5.23	5.59	5.1
	22	4-Decylaniline	***4.8***	(5.45)		3					(−)	6.75	6.2
2°	23	*N*-Methylbenzylamine	9.5	0.91	0.06	2	1.01	0.00	3	0.10	1.01	0.80	1.5
	24	*N*-Ethylbenzylamine	9.6	0.63		1	1.14	0.01	3		1.14	0.72	2.1
	25	*N*-Butylbenzylamine	***9.9***	1.56	0.06	2	1.69	0.01	3	0.13	1.69	1.43	3.1
	26	*N*-Hexylbenzylamine	***9.9***	2.46	0.00	3	2.52	0.00	2	0.06	2.52	2.30	4.2
	27	*N*-Octylbenzylamine	***9.9***	3.61		5					3.73	3.05	5.2
	28	3-Methyl-*N*-Methylbenzylamine	***9.7***	1.35	0.05	2	1.46	0.00	3	0.11	1.46	1.23	2.0
	29	Methamphetamine	9.9	1.43	0.00	2	1.56	0.00	3	0.14	1.56	1.16	1.9
	30	*N*-methylphenethylamine	10.1	1.20	0.05	2	1.30	0.00	3	0.10	1.30	1.17	1.6
	31	Dibenzylamine	***9.1***	2.08		1	2.18	0.00	3	0.10	2.18	1.57	3.4
	32	Dicyclohexylamine	***11.1***				1.86	0.01	3		1.86	1.11	3.7
	33	Dihexylamine	***10.8***				2.78	0.01	3		2.78	2.44	4.9
	34	*N*-Ethylcyclohexylamine	***10.8***				1.06	0.01	3		1.06	0.47	2.2
	35	*N*-Methyloctylamine	***10.5***				2.33	0.00	3		2.33	2.62	3.3
	36	*N*-Methyldodecylamine	***10.5***				4.81		4		4.81	4.87	5.4
	37	Maprotiline	10.2				3.80		3		3.80	3.36	4.5
	38	*N*-Methylaniline	4.9	0.84		1					0.96	0.61	1.6
	39	*N*-Ethyl-*M*-toluidine	5.3	1.45		1					1.57	1.03	2.6
3°	40	Pyridine	5.2	−0.16	0.07	3					−0.04	−0.66	0.7
	41	Quinoline	4.9	1.16	0.01	2					1.28	−0.10	2.1
	42	Acridine	6.2	2.12		1					2.24	0.33	3.4
	43	2-Methylpyridine	6.0	−0.15		1					−0.03	−0.74	1.2
	44	2-Ethylpyridine	5.9	0.29		1					0.41	−0.43	1.7
	45	3,4-Lutidine	6.5	0.18		1					0.30	−0.12	1.7
	46	2,6-Dimethylpyridine	6.6	0.44		1					0.55	−0.80	1.7
	47	2,4,6-Collidine	7.4	0.66		1					0.78	−0.34	2.1
	48	*N*,*N*-Dimethylbenzylamine	8.9	0.90		1	1.08	0.00	3	0.19	1.08	0.38	2.0
	49	*N*,*N*-Diethylbenzylamine	***9.5***	1.17		1	1.36	0.01	3	0.18	1.36	0.35	3.0
	50	*N*,*N*-Dimethyloctylamine	***9.8***				2.35	0.00	3		2.35	2.21	3.8
	51	*N*,*N*,*N*-Tributylamine	10.9				1.92	0.01	3		1.92	1.89	4.8
	52	*N*,*N*,*N*-Trihexylamine	***10.8***				4.67		4		4.67	4.64	8.0
	53	*N*,*N*-Dimethylcyclohexylamine	***10.2***				1.04	0.01	3		1.04	0.14	2.1
	54	*N*,*N*-Diethylaniline	6.6	1.20		1					1.32	0.24	3.4
	55	Imipramine	9.4	3.60		5					3.72	2.60	4.8
	56	Amitriptyline	9.4	3.79		5					3.91	3.34	4.9
	57	Fenpropidin	10.1	3.57		4					3.69	2.93	5.9
4°	58	Octyltrimethylammonium	—				2.18	0.00	3		2.18	1.92	—
	59	Decyltrimethylammonium	—				3.17	0.00	2		3.17	3.04	—

Table 1 (*Contd.*)

Amine type	#	Chemical name	pK_a[a]	log K_{IAM} pH 3.0 *50*	Diff[b]	*N*	log K_{IAM} pH 5.0 *46*	Diff[b]	*N*	ΔpH_{5-3}[c] *26*	log K_{PLIPW} Cation	log K_{DMPC} Cation	log P[e] Neutral
	60	1-Butylpyridinium	—	0.70		1	0.91	0.01	3	0.20	0.91	0.05	—
	61	MPP^+	—	1.43		1	1.61	0.00	3	0.18	1.61	0.37	—
	62	Phenyltrimethylammonium	—				0.74	0.01	3		0.74	−0.31	—
	63	Benzyltrimethylammonium	—	0.83	0.08	3	0.93	0.01	3	0.10	0.93	−0.06	—
	64	Benzyltriethylammonium	—	1.23	0.06	2	1.47	0.01	3	0.24	1.47	0.37	—
	65	Benzyltripropylammonium	—	1.80	0.05	2	1.96	0.01	3	0.16	1.96	1.75	—
	66	Benzyltributylammonium	—	2.49		1	2.63	0.01	2	0.14	2.63	3.33	—
	67	Benzyldimethylhexylammonium	—	2.31	0.00	2	2.42	0.00	2	0.11	2.42	1.69	—
	68	Benzyldimethyloctylammonium	—	3.19		1	3.30	0.00	2	0.11	3.30	2.81	—
	69	Benzyldimethyldecylammonium	—	4.35		5					4.47	3.89	—
	70	Benzyldimethyldodecylammonium	—	5.5		2					(5.6)	4.98	—

[a] pK_a values are experimental data from SRC/EPISuite (maprotiline, Cabot *et al.*, 2014: ref. 26), with bold-italic values predicted by http://www.chemicalize.org (July 2015). [b] Maximum difference between log K_{IAM} measurements. [c] For 26 amines measurements were made in both pH 5.0 and pH 3.0 eluents, ΔpH_{5-3} expresses the difference (average 0.12 ± 0.05). With negligible electrostatic effects at pH 5.0 (Droge, 2016: ref. 16), the intrinsic log K_{PLIPW} for cationic species is set equal to the log K_{IAM} at pH 5.0 for bases with pK_a > 7. For weak bases with pK_a between 3.8 and 7, measurements at pH 3.0 were used to determine the intrinsic log K_{PLIPW} for cationic species incl. ΔpH_{5-3}. [d] Two peaks were identified with the same *m*/*z* for 4-*t*-tylcyclohexylamine. [e] log *P* values are predictions from ACD/Labs software.

corresponding to physiological salinity (0.15 M) and composition of phosphate buffered saline (PBS) solution. The aqueous eluent used for LC-MS detection consisted of only 10 mM buffer (ammonium acetate at pH 5.0, phosphoric acid at pH 3.0). The influence of different buffer and salinities at pH 5.0 on IAM-retention was tested with UV-detection for several compounds with UV-absorbing moieties and compared with IAM retention on LC-MS. Triplicate IAM-injections were run on the same day for most compounds. Series of at least 3 different eluent mixtures with acetonitrile (≤30% acetonitrile) were applied to strongly sorbing amines and extrapolated to obtain the $K_{IAM,app}$ values for 100% aqueous buffer. For some amines, higher acetonitrile fractions were applied for range-finding purposes.

2.3 HPLC detection and analysis

An Agilent 1100 Diode-Array UV system was set to simultaneous detection of 207, 220, 254, and 278 nm for each compound with UV-absorbing moieties, in order to confirm peaks of the test compounds. For amines lacking UV-absorbing moieties, an MDS Sciex API 2000 LC-MS/MS system (Applied Biosystems, Foster City, CA, USA) was used, using a Perkin Elmer (Norwalk, CT, USA) liquid chromatography system. The Turbo Ion spray source was set in positive mode at 1500 V and operated at 400 °C, with only a <5% split volume of the 1 mL min^{-1} flow injected. Scans were performed on parent *m*/*z* characteristics [MH^+]. 3-Nitroaniline was the neutral reference compound to check IAM consistency during UV-diode array detection. Pure water (MilliQ, Millipore Merck) was used as a neutral non-retained tracer (t_0) on UV-diode array detection. Tryptamine was used as a reference cation to align retention on UV-diode array and LC-MS systems. The peak apex of the eluted peak (t_r) on both detectors was used to calculate retention capacity factors (k_{IAM}) based on the ratio $t_r/(t_r - t_0)$. The intrinsic phospholipid sorption coefficient (K_{PLIPW} (IAM)) at pH 5.0 was obtained by multiplying k_{IAM} by the solvent/sorbent phase ratio of 18.9 for the IAM.PC.DD2 column.[16,17] In pH 3.0 eluents, used to determine $K_{PLIPW,ion}$ for several bases with pK_a of 5–7, the IAM surface becomes positively charged which decreases the apparent retention of cations.[16] Additional measurements for several fully charged bases (pK_a > 7) were performed at both pH 3 and pH 5 at a salinity of 0.15 M, to confirm our previously established compensation factor of 0.12 log units to translate the apparent $K_{IAM(pH3)}$ to K_{PLIPW}(IAM).[16]

2.4 Molecular simulations

COSMOmic was run within COSMOtherm Version C30_1501, using the time average 1,2-dimyristoyl-*sn*-glycero-3-phosphocholine (DMPC) micelle file COSMOmic-dmpc.mic provided with this version, obtained with molecular dynamics (MD) simulation as described previously,[15] along with TZVP-optimized structures of water and a representative DMPC phospholipid molecule. The COSMOmic default "self-defined" electrostatic potential was used (position 17.0796, width 8.86629, depth 7.51583 kcal (326 mV)). These are the same time-averaged micellar composition and optimized potential settings according to Bittermann *et al.*[11] COSMOmic divides the average atomic distribution in the MD simulated DMPC bilayer into 31 layers for one half of the hydrated bilayer, and calculates the free energy for each chemical input structure at 162 orientations. The surface charge density of the three dimensional input structures is quantum-chemically optimized at TZVP level for calculations with COSMOtherm, and calculations with different conformers were combined by COSMOmic using weightings from statistical mechanics. COSMOconf conf Version 3.0.0.0 was used to create up to 6 of the most relevant conformers for all charged amines, in a pre-defined stepwise protocol (selection

steps at different levels of parameterization of maximum 100 (loose SVP), 40 (SVP), 8 (TZVP), 6 (final TZVP) structures), applying TurbomoleX13.

3. Results and discussion

3.1 IAM-HPLC data generation

Triplicate sampling on different days with the same buffer resulted in apparent log K_{IAM} values that differed by less than 0.05 (Table 1). Most of the data were generated using the "ideal" IAM-HPLC eluent, with negligible confounding electrostatic effects in high saline pH 5.0 buffer as discussed in a previous study,[16] so that the apparent log K_{IAM} values were directly related to the intrinsic K_{PLIPW} for the cationic species of bases with a pK_a > 8. However, 13 of the 69 amines have a pK_a between 3.9 and 7.2. Along with many other amines, these 13 amines were also tested in highly saline pH 3.0 buffered eluent. Using data on 26 bases with a pK_a > 8 tested at both pH 5 and pH 3 eluents, the average log K_{IAM} difference ($\Delta\log K_{pH5-3}$) is 0.12 ± 0.05 (Table 1), closely corresponding to the findings in the recent IAM-HPLC study where a correction value of 0.15 was applied.[16] Assuming that the apparent log K_{IAM} obtained at pH 3.0 for the weaker bases with pK_a 3.9–7.2 were not influenced by the relatively small fractions of corresponding neutral species (see Section 3.2.4), all log K_{IAM} values generated at pH 3.0 are converted to intrinsic K_{PLIPW}(IAM) values of cationic species by addition of 0.12 log units.

Since the confounding influence of salinity on IAM-retention of organic cations is negligible at pH 5.0,[16] different buffers can be readily used at this pH, even at lower ionic strength. Instead of high concentrations of non-volatile salts in PBS, 10 mM ammonium acetate (NH_4Ac) buffered eluent could thus be used to apply LC-MS as an alternative detection method for the amines lacking UV-absorbing moieties. ESI-Fig. S2† shows data for the neutral reference 3-nitroaniline and six cations on different detectors. With UV detection, K_{IAM} values differ by less than 0.1 log unit when the pH 5.0 eluent contains 0.015–0.15 M NaCl, or 0.01–0.03–0.15 M NH_4Ac (ESI-Fig. S2†), and LC-MS detection shows consistent results in 0.01 M NH_4Ac. This allowed the generation of K_{IAM} data for the 20 amines that lack UV-absorbing moieties, including cyclohexanamines, (branched) alkylamines, amantadine, and fenpropidin. In case of chemical impurities that show additional peaks on the UV-chromatograms, LC-MS specifically targeted compounds by their mass detection. Alternatively, 4-*tert*-butylcyclohexyl-amine (compound #9) showed two distinct peaks on the LC-MS with the same *m*/*z* ratio, apparently these were isomers with slightly different sorption affinities (0.15 log units difference in log K_{IAM}, value is averaged in Table 1).

For the 16 amines with relatively high affinity for the IAM-column, a series of multiple eluent mixtures of saline pH 3.0 or 5.0 buffers with acetonitrile were tested in order to extrapolate to apparent K_{IAM} values in fully aqueous buffer (ESI-Fig. S3†). For 14 of these amines, eluents with ≤30% acetonitrile incremented in steps of 5% were sufficient for extrapolation. Benzyldimethyloctylammonium (#68) indicated a linear extrapolation between 100% aqueous eluent up to 30% acetonitrile. Data for many other amines obtained at ≥30% acetonitrile tended to underestimate the extrapolated K_{IAM} value (ESI-Fig. S3†) compared to our previous IAM study.[16] For 4-decylaniline (#22) and benzyldimethyltetradecylammonium (not listed) only data at ≥30% solvent could be measured, hence extrapolation to fully aqueous eluent was highly uncertain.

3.2 COSMOmic data

The average of the number of conformers generated for each $C_xH_yN^+$ amine was 3.2, with 18 out of 70 amines having only a single conformer (ESI-Table S2†). For amines with multiple conformer structures, the average difference between the conformer specific log K_{DMPC}(COSMOmic) is 0.46 log units, ranging between 0 and 1.15 log units. As an example, the highest log K_{DMPC} difference (1.15) between conformers was for the 1° amine 3-phenylpropylamine (#7), where the propylamine chain is either stretched away from the aromatic ring, or curled so that the charged amine approaches the aromatic ring (ESI-Fig. S4†). The weighted conformer log K_{DMPC}(COSMOmic) for 3-phenylpropylamine indicates negligible influence of the curled conformer. The weighted conformer partition coefficients are used throughout the following evaluations in this study.

COSMOmic provides several examples of bilayer systems. Using the DMPC and 1-palmitoyl-2-oleoyl-*sn*-glycero-3-phosphocholine (POPC) optimized membrane potential settings suggested by Bittermann *et al.*,[11] the simulated K_{PLIPW} values for POPC are on average 0.98 log units (s.d. 0.30) higher than those for DMPC (ESI-Fig. S5†). Although this may be related to the slightly different distributions of the anionic phosphate and cationic ammonium groups in the two systems (ESI-Fig. S5†), the membrane potential settings were fitted in Bittermann *et al.*[11] according to reference values for the same cationic and anionic structures in both systems. Interestingly, compounds that show very little difference (0–0.5 log units) between POPC and DMPC predictions are all amines surrounded by multiple alkyl chains (*e.g. N*,*N*,*N*-trihexylamine #52, benzyltributylammonium #66), indicating that the composition of the simulated bilayer system can influence the contribution of distinct structural solute features. COSMOmic predictions for organic cation structures are also influenced by the applied input structure of a representative phospholipid molecule (data not shown),[18] but we chose to apply the original software settings and did not aim to optimize this further. Comparing the K_{PLIPW}(IAM) values for all $C_xH_yN^+$ amines with the COSMOmic predictions (ESI-Fig. S5†), POPC predictions are all too high, while DMPC predictions are in line with the IAM-HPLC data (Fig. 1). We therefore focus further comparisons of IAM-HPLC data on simulations with the DMPC system.

3.3 IAM-HPLC data interpretation

As shown in Fig. 1, the sorption affinity of $C_xH_yN^+$ amines generally increases for structures with more carbon units (#C in left graph). However, this approach neglects different influences between aromatic hydrocarbon units, branched structures, and alkyl chains. Decylamine (#13) and amantadine (#16) are both primary amines with 10 carbon atoms, but

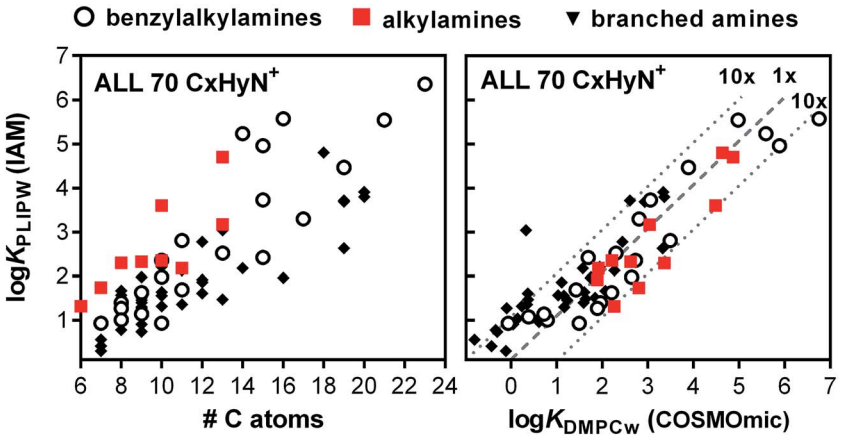

Fig. 1 IAM-HPLC based phospholipid sorption coefficients for all tested $C_xH_yN^+$ compounds plotted against number of carbon atoms (#C, left) or simulated DMPC sorption coefficients (COSMOmic log K_{DMPC}, right). Broken lines in the right column indicate 1 : 1 relationship between observed and predicted sorption coefficients, dotted lines 10× higher or lower differences.

log K_{PLIPW}(IAM) values differ by 2 units (3.60 and 1.64, resp.). As shown in the right plot of Fig. 1, calculated log K_{DMPC} values with COSMOmic could serve as reasonable predictions, with nearly all compounds within a factor of ±10 of the IAM-HPLC based K_{PLIPW} (see eqn (2) in Table 2 for regression details). To illustrate, COSMOmic predicts 2.9 log units difference between decylamine and amantadine. The consistent IAM-HPLC based K_{PLIPW} data on 70 $C_xH_yN^+$ amines contains rich subsets of chemicals that allow evaluation of the influence of amine type, alkyl chain length, position of the charged moiety in the molecule, branching, and presence of aromatic rings, on the sorption affinity to a membrane. This approach may render values for the contribution of different CH_x fragments to K_{PLIPW}. Furthermore, for each subset, the observed trends in experimental data can be compared to those in the quantum-chemical based software predictions with COSMOmic, and those in the octanol-water partition coefficients as a classical lipophilicity descriptor.

Table 2 Regression analysis of IAM-HPLC based log K_{PLIPW} values with COSMOmic log K_{DMPC}, log P values (ACD/Labs estimates), molecular volume (Vx), and amine type corrective increments

COSMOmic DMPC bilayer (1° to 3°)								
#	a log K_{DMPC}	$+c$				sy.x	df	<3x^d
Eqn (1)	0.72(0.05)[a]	0.71(0.12)[a]				0.57	55	67
COSMOmic DMPC bilayer (1° to 4°)								
#	a log K_{DMPC}	$+c$				sy.x	df	<3x^d
Eqn (2)	0.73(0.04)[a]	0.76(0.10)[a]				0.57	68	74
	a log K_{DMPC}	$+\delta1°$[b]	$+\delta2°$	$+\delta3°$	$+\delta4°$			
Eqn (3)	1.0[c]	−0.51 (0.13)	0.34 (0.14)	0.76 (0.14)	0.68 (0.11)	0.36	67	83
ACD/labs log P (1° to 3°)								
#	a log P	$+c$				sy.x	df	<3x^d
Eqn (4)	0.77(0.05)[a]	−0.22(0.18)[a]				0.60	55	63
	a log P	$+\delta1°$[b]	$+\delta2°$	$+\delta3°$				
Eqn (5)	1.0[c]	−0.35 (0.17)	−1.03 (0.18)	−1.50 (0.13)		0.51	54	78
Molecular volume (1° to 3°)								
#	aVx	$+c$				sy.x	df	<3x^d
Eqn (6)	2.50(0.19)[a]	−1.59(0.29)[a]				0.66	55	70

[a] Coefficients a and c with standard errors between parentheses. [b] δ represents the amine type specific corrective increments on log K_{DMPC} values (with standard error margins). [c] Without acridine and benzyltributyl-ammonium, using a fitted linear curve with a slope of 1.0. [d] Percentage of compounds with fitted value less than a factor of 3 different from observed K_{PLIPW}. sy.x is the standard deviation of the residuals.

A more detailed evaluation of subsets of chemicals could elucidate features that can be adequately represented by descriptors, and those that are responsible for scatter in regression against experimental data. In addition, we use the COSMOmic output for information about the favourable depth and 3-dimensional orientation of sorbates in the hydrated phospholipid bilayer to provide a better understanding of data trends for analogue series.

3.3.1 Fragment value for CH_3 units directly attached to the ionizable nitrogen. Different amine types are distinguishable based on the number of methyl groups attached to the charged nitrogen. The coloured COSMOtherm input structures for the benzylamines in Fig. 2 illustrate that methylation of the amine results in a different distribution of the charge on the molecular surface, as noted previously.[19] Primary amines (*e.g.* benzylamine, furthest left in Fig. 2) have a large area of high surface charge (purple colour = high positive surface charge) covering the entire NH_3^+ unit, while the 1+ surface charge of the nitrogen in the quaternary benzyltrimethyl-ammonium (most right structure in Fig. 2) is fully distributed over the attached methyl groups (light blue colour = very low positive surface charge). The IAM-HPLC based log K_{PLIPW} values do not differ more than 0.1 log unit for different amines types with a similar hydrocarbon side structure, either octyl-chains or benzyl-units (Y-axis in Fig. 2). The CH_3-groups connected to the charged nitrogen

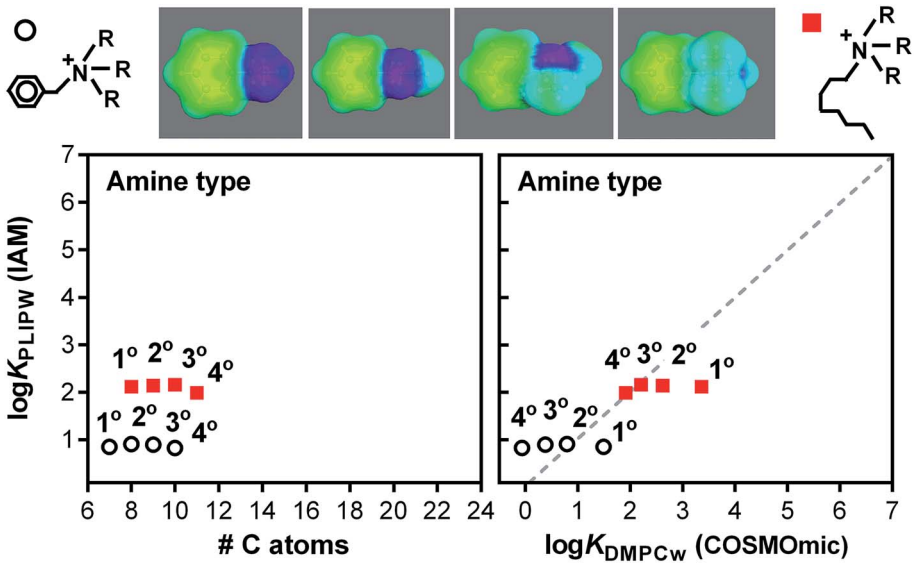

Fig. 2 IAM-HPLC based phospholipid sorption coefficients for analogue $C_xH_yN^+$ compounds with different amine types, plotted against number of carbon atoms (#C, left) or simulated DMPC sorption coefficients (COSMOmic log K_{DMPC}, right). Red squares a series of 1° to 4° octylamines (R = H or CH_3) and circles are 1° to 4° benzylamines (R = H or CH_3). The effect of amine type on surface charge density (dark blue/purple = very low electron density (positive charge); green = neutral surface charge, yellow = slightly increased electron density) is shown in COSMOmic input structures above the graphs.

apparently do not contribute to the overall sorption affinity to the phospholipid coating. This strongly contrasts with experimental log *P* values of *e.g.* different benzylamines, which increase about a log unit from primary (1.09), secondary (1.52), and tertiary amine analogues (1.98).[20] Conversely, COSMOmic predicts a stepwise reduction of the sorption affinity from 1° amines to 3° amines, probably due to the increased focusing of the 1+ charge onto a smaller surface area, and strong charge distribution and even lower affinity in 4° amines (right plot Fig. 2). Despite the three additional methyl groups on the quaternary amines, COSMOmic predicts 1.5 log units higher affinities for analogue primary amines, for both alkylamines and benzylamines, both in DMPC and in POPC bilayer systems. This does not match the IAM-HPLC data. COSMOmic thus overestimates primary amines and underestimates quaternary ammonium compounds compared to IAM-HPLC based log K_{PLIPW} (also discussed below in Fig. 3).

An underestimation of the effects of methylation on the amine by COSMOmic, and overestimation by log *P*, directly introduces substantial scatter between experimental and descriptor based regressions if all different types of amines are used in a comparison, as shown in Fig. 1. Still, it is not yet clear whether this discrepancy between IAM-HPLC data and COSMOmic predictions are the result of a flaw of the molecular simulations, or a misrepresentation of partitioning into liposome membranes by the phospholipid monolayer coating in IAM-HPLC. In the absence of large experimental partitioning data sets of $C_xH_yN^+$ amines on dispersed liposomes, we regard the IAM-HPLC data as reliable interpretations of artificial membrane affinities, also regarding the successful comparison on 14 amine structures in the preceding IAM-HPLC study.[16]

3.3.2 Fragment value for CH_2 units in a linear alkyl chain. There are several series of analogue amines tested that only differ in the length of linear alkyl chains, shown in Fig. 3. For primary amines, we tested alkylamines and several types of alkylbenzylamines, with alkylchains attached either on the *para*-position of the aromatic ring in an aniline or benzylamine group, or in between the aromatic ring and the primary amine. For quaternary ammonium compounds, a series of benzalkonium structures is included with alkyl chains ranging from C_1–C_{14}, and two alkyltrimethylammonium compounds (C_8 and C_{10}). Plotted against the number of C-atoms in each amine, as shown in Fig. 3, log K_{PLIPW}(IAM) values for these series increase with slopes between 0.49 and 0.58. This corresponds to, or is even slightly higher than, the influence of C_2H_4 increments in liposomal partitioning data for neutral compounds, *e.g.* log K_{PLIPW} differed 0.87 between hexane/octane,[10] and 1.18 between 1-butanol/1-hexanol and 0.94 between 1-hexanol/1-octanol (Busella 1996, cited in ref. 10).

COSMOmic predicts the most favourable molecular orientation in the different regions of the membrane. The original COSMOmic output files of the ideal orientation are presented for several $C_xH_yN^+$ amines in ESI-Fig. S6.† The 3D graphs are simplified for some compounds in Fig. 4 by leaving out the coloured membrane sections and background, focusing only on the sorbate structure. Fig. 4 also shows that the phosphate anions of the phospholipids in hydrated DMPC membrane occur mostly in the range between 15 and 20 Å from the core of the simulated membrane. According to the most favourable orientation of *N*-methyldodecylamine (#36, Fig. 4), the cationic nitrogen is positioned in the phosphate anion rich region of the headgroups, and the linear alkyl chain extends into the hydrophobic core of the bilayer. The contribution of additional CH_2

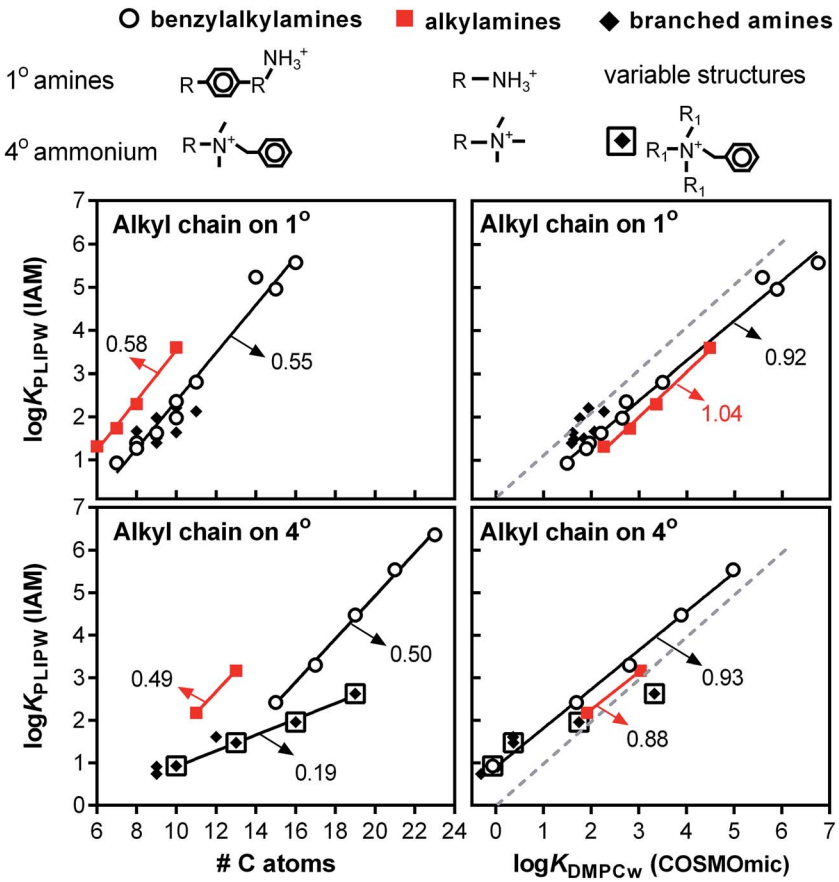

Fig. 3 IAM-HPLC based phospholipid sorption coefficients for analogue $C_xH_yN^+$ compounds with different alkyl chain lengths, plotted against number of carbon atoms (#C, left) or simulated DMPC sorption coefficients (COSMOmic log K_{DMPC}, right). Examples of the compounds included are drawn above the figures, where R denotes an alkyl chain, and R_1-groups in the branched quaternary ammonium structure (boxed diamonds) are of equal length for each compound in the tested series. The values with each arrow are the slopes of the plotted regressions.

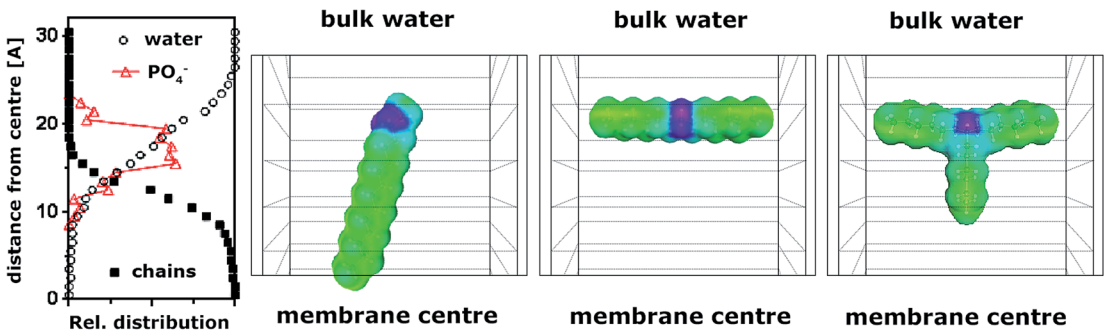

Fig. 4 Distribution of water molecules, alkyl chains and phosphate anions in COSMOmic's DMPC membrane (graph left), and schematic representation of most favourable 3D-orientation of three $C_xH_yN^+$ amines in DMPC membrane calculated by COSMOmic (all zoomed in, bulk water much higher, bilayer center much lower relative to the graph on the left). From left to right: *N*-methyldodecylamine (#36) aligns almost vertically parallel to phospholipids, dihexylamine (#33) aligns horizontally within the phosphate rich headgroup domain, *N*,*N*,*N*-trihexylamine (#52) extends with one chain into the hydrophobic core of the bilayer. Green alkyl chains are electroneutral, the cationic nitrogen unit is purple.

units in such alkyl chains of organic cations is similar to those in neutral compounds. For these single chain amines COSMOmic also predicts CH_2 increments of ~0.5 log units (Fig. 3). Conformers of *N*-methyldodecylamine with a slightly coiled alkyl chain have 0.43 log units lower K_{DMPC} predictions than fully extended conformers, but all still with the alkyl chain extended in the hydrophobic core (ESI-Fig. S7†). Interestingly, the primary amine 4-octylbenzylamine (#4) sorbed much stronger than it's close secondary amine analogue *N*-octylbenzylamine (#27) (log K_{PLIPW}(IAM) of 5.0 and 3.7, respectively). COSMOmic predictions (log K_{DMPC} of 5.9 and 3.0) elucidate that this is mainly due to the fully external position of the charged

amine in 4-octylbenzylamine (#4), which therefore sorbs at a distance (for the molecular centre) of only 8.5 Å from the bilayer's centre, while *N*-octylbenzylamine (#27) sorbs at @11.5 Å (Fig. S6†), closer to the phosphate rich region headgroup to better align the charge–charge interactions. As discussed below, log K_{PLIPW} values for $C_xH_yN^+$ amines with multiple linear alkyl chains attached to the charged nitrogen are considerably lower than expected based on these results for single alkylchain cations. The simulated favourable orientation and depth within the phospholipid membrane of $C_xH_yN^+$ amines with COSMOmic aids in understanding these effects.

3.3.3 Effect of favourable position and orientation inside phospholipid membranes. According to the COSMOmic simulations for nearly all of the evaluated $C_xH_yN^+$ amines, the charged nitrogen moiety resides favourably in the phosphate rich region (see PO_4^- distribution in Fig. 4). The energetically optimal orientation and position of the whole $C_xH_yN^+$ amine inside the phospholipid bilayer depends on the length of the different side groups surrounding the charged nitrogen. The longest chain tends to be positioned towards the hydrophobic core. As a result the methyl-group in *N*-methylalkylamines is in the headgroup area (Fig. 4). Dihexylamine has two equally long alkyl chains with the nitrogen exactly in the middle of the molecule. The IAM-HPLC based log K_{PLIPW} of dihexylamine (#33) is 2 log units smaller (4.8 *vs.* 2.8) than that of *N*-methyldodecylamine (#36) while the latter compound has only 1 extra CH_2 unit. The most favourable orientation and position calculated with COSMOmic for dihexylamine is with both alkyl chains in the same headgroup layer where the phosphate anions reside (Fig. 4), as well as ammonium groups, water, and glycerol ethers. The alkyl chains positioned in the headgroup area may disturb many polar/charge interactions between surrounding molecular units, reducing the free energy gain from removal of hydrophobic CH_x units out of water, especially compared to positioning into the hydrophobic core where mostly van der Waals forces occur between neighbouring atoms. Furthermore, the alignment of an alkyl chain alongside the tails of the phospholipids may cause less strain on the phospholipid ordering than taking up the space between several phospholipid headgroups. The same horizontal positioning is predicted for all six conformers of dihexylamine, with a maximum 0.41 difference in log K_{DMPC} (ESI-Fig. S8†). Taking this difference in location between dihexylamine and *N*-methyldodecylamine into account, COSMOmic adequately approaches the experimental difference between the two compounds (2.4 log units smaller log K_{DMPC} for dihexylamine). *N*,*N*,*N*-Trihexylamine (#52) is predicted by COSMOmic to have two alkyl chains stretched horizontally in the headgroup plane, and one chain extended into the hydrophobic core (Fig. 4). Compared to dihexylamine, the six additional carbon atoms increase the IAM-HPLC based log K_{PLIPW} by 1.8 log units (2.8 *vs.* 4.6), an average increment of each carbon atoms in the third alkyl-chain of 0.3. This difference between dihexylamine and *N*,*N*,*N*-trihexylamine is again adequately predicted by COSMOmic log K_{DMPC} values (2.4 *vs.* 4.6). This evaluation shows that the contribution of a CH_2 fragment to the log K_{PLIPW} strongly depends on the position of each side group of the charged nitrogen in the phospholipid bilayer.

If a charged secondary amine has a more hydrophobic domain on one side than the other, the contribution of the CH_x units may significantly differ from one side to the other. For smaller $C_xH_yN^+$ amines, these effects are of course reduced, but they explain the differences between *N*-alkylbenzyl-amine analogues. If the *N*-alkylchain increases from methyl (log K_{PLIPW}(IAM) 1.01, phenyl ring towards centre of bilayer) to ethyl, (log K_{PLIPW}(IAM) increases only 0.13 log units), to butyl (horizontal positioning), to octyl (alkyl chain towards centre of bilayer) (ESI-Fig. S6†). Because of the different orientations between amines in this series, the average CH_2 contribution gradually increases. COSMOmic even predicts a slightly lower K_{DMPC} for ethyl compared to a methyl side group (Table 1). An even more extreme trend was noted in liposomal partitioning experiments with (*p*-methylbenzyl)-alkylamines, where cation partition coefficients showed a decreasing trend between "no methyl"-methyl-ethyl-propyl groups as alkyl moiety (full log unit difference), and only an increase in partition coefficient from butyl and longer chains.[21]

Also for the quaternary ammonium compounds a series was examined where the amine was centred in the molecule; the four benzylammonium compounds with either trimethyl, triethyl, tripropyl or tributyl groups on the charged nitrogen (#63–66). The extension of all three alkyl chains with a CH_2 unit in these compounds resulted in an even lower average contribution of a single CH_2 unit of 0.19 log units as compared to *N*,*N*,*N*-trihexylamine (see trend in bottom left plot of Fig. 3). These trialkylbenzylammonium compounds also showed a lower CH_2 increment value than linear (benzyl)alkylamines in sorption studies to soil organic matter and clay.[19,22] The COSMOmic K_{DMPC} predictions follow this trend between benzyltrimethylammonium (#63) and benzyltriethylammonium (#64), but at longer alkyl chains the predicted increments are overestimated. Extended branching on the charged nitrogen may cause a more diffuse distribution of surface charge than accounted for by the COSMOmic input structures or sigma-profile calculations.

Overall, the evaluation of the effect of the position of the charged amine clearly demonstrates benefits of including calculations for different orientations combined with quantum chemistry based software calculations like COSMOmic. The anisotropic structuring of phospholipid membranes and the strong effect of the orientation of the $C_xH_yN^+$ amines in the membranes limits log *P* based approaches. log *P* based regressions for K_{PLIPW} fail to pick up the ~2 log unit difference between dihexylamine (#33) and *N*-methyldodecylamine (#36) (difference 0.5 log units using log *P* (ACD/Labs) 4.9 and 5.4, respectively). Since the contribution of CH_x groups in organic cations to the overall membrane affinity strongly depends on the most favourable orientation and position of the molecule in the bilayer, and the resulting position of the CH_x group it is also not possible to define a single increment value for different types of CH_x in a molecular fragment approach.

3.3.4 COSMOmic performance on branched amines and aromatic structures. The performance of COSMOmic on branched structures can be well evaluated by comparing trends between sets of linear and branched amines, and those with

and without aromatic rings. 1-Octylamine (#12, log K_{PLIPW} 2.3) sorbs 0.8 log units stronger than *tert*-octylamine (#14, log K_{PLIPW} 1.5). COSMOmic accounts for branching, but seems to strongly exaggerate the effect on K_{DMPC}. K_{DMPC} predictions are 1.7 log units lower for *tert*-octylamine (3.35 *vs.* 1.64), even though the chains of both amines are positioned towards the hydrophobic core. Smaller differences due to branching with only a single methyl group occur between C_8-isomers amphetamine (#6) and 3-phenylpropylamine (#7), with 0.14 log units lower K_{PLIPW}-(IAM), and 0.36 log units lower K_{DMPC}(COSMOmic), for amphetamine. Fig. 3 shows that differences between alkyl, benzylalkyl and branched structures for the whole set of primary amines or quaternary ammonium compounds are strongly reduced in the COSMOmic predictions compared to simply comparing by the number of carbon atoms. The COSMOmic predictions only start to deviate substantially from IAM-HPLC based K_{PLIPW} values for strongly highly branched structures. In addition to differences between the two earlier mentioned primary amines with 10 carbon atoms (decylamine and amantadine), COSMOmic also closely resembles the IAM-HPLC trend for other primary amines C_{10}-isomers (Fig. 5): decylamine (#13) > 4-*tert*-butylcyclo-hexylamine (#9) > 4-phenylbutylamine (#8) ~ naphthylamine (#18) > amantadine (#16), indicating reasonable performance for both branched and aromatic structures compared to linear analogues.

Also shown in Fig. 5 are several polyaromatic amines. The weak base naphthylamine (#18, pK_a 3.92) has an almost equal log K_{IAM} at pH 3.0 compared to the strong base 1-naphthylmethylamine (#17, pK_a 9.05), despite having one methyl group less (Table 1). Since at pH 5 and pH 7.4 the neutral naphthylamine species are dominant, IAM-HPLC at those pH values is not impacted by electrostatic effects. IAM-HPLC measurements at pH 3.0, 5.0 and 7.4, were fitted to the Henderson–Hasselbalch equation[23] with pK_a fixed at 3.92 (ESI-Fig. S9†). The resulting fit suggests a minor influence of neutral species at pH 3.0, and a log $K_{IAM,cation}$ of 1.80, instead of the apparent log K_{IAM} of 2.09. The CH_2 unit between the ring and the charged amine in 1-methylnaphthylamine still contributes only 0.14 log units. Quinoline (#41, pK_a 4.9) has the charged amine as part of a double aromatic ring, and 98.6% of the compound are cationic species at pH 3.0. Quinoline has only one aromatic CH unit less than naphthylamine, which in this case results in a log K_{PLIPW} 0.67 log units lower (1.28 *vs.* 1.95). This may be due to the charge delocalization in the aromatic rings, but other studies applying COSMOtherm have also noticed that neutral polyaromatic compounds were systematic outliers in predictions for partitioning to octanol and liposomes.[10,11] COSMOmic predictions closely resemble the differences between most of these sets of amines with/without aromatic rings, but deviates for the N-heterocyclic amines. The tricyclic aromatic amine acridine (#42) appears to be the most problematic $C_xH_yN^+$ compound in our data set for COSMOmic K_{DMPC} predictions (2.5 log units lower than IAM-HPLC K_{PLIPW}).

3.4 Single-parameter regressions for the K_{PLIPW} of $C_xH_yN^+$ amines

Accounting for optimized sorbate orientation and inclusion of conformers clearly improves the predictive power of COSMOmic for specific structures compared to the bulk phase partition constant log *P*. This leads to the question: does including COSMOmic calculations in a regression improve the overall performance of models for the membrane affinity of organic cations compared to other descriptors? Table 1 lists the experimentally derived log K_{PLIPW} values and the simulated log K_{DMPC} values for $C_xH_yN^+$ species, as well as the predicted log *P* values for corresponding neutral species (ACD/Labs log *P*, does not calculate values for the quaternary ammonium structures). Since $C_xH_yN^+$ compounds lack functional groups other than aromatic rings, we also evaluated the performance of a simple molecular volume descriptor (McGowan's Vx) to assess overall differences in membrane affinity due to simple structural features (compared to simply the number of carbon atoms, ESI-Fig. S10†).

As displayed in Fig. 1, there is still substantial scatter (mostly within a factor of ±10) between K_{PLIPW} values of $C_xH_yN^+$ amines and COSMOmic predicted log K_{DMPC} values. Using all 68 tested compounds, the log K_{PLIPW} *vs.* log K_{DMPC} regression has a slope of 0.73 (±0.04 s.e.), sy.x (standard deviation of the residuals) = 0.57 log units, and R^2 = 0.83. Table 2 shows all regression details. When excluding the quaternary ammonium compounds (eqn (1) in Table 2, sy.x = 0.57, N = 57), the COSMOmic based regression is not an improvement over the regression between log K_{PLIPW} and log *P* values (eqn (3), sy.x = 0.60) predicted with ACD/Labs software. Without the outlier acridine (#42), the COSMOmic regression is considerably improved (sy.x = 0.50) (Fig. 6 and ESI-Fig. S11† shows fitted values based on the log *P*-regression and comparison with ACD/Labs predicted log $D_{5.5}$ values). Without the quaternary

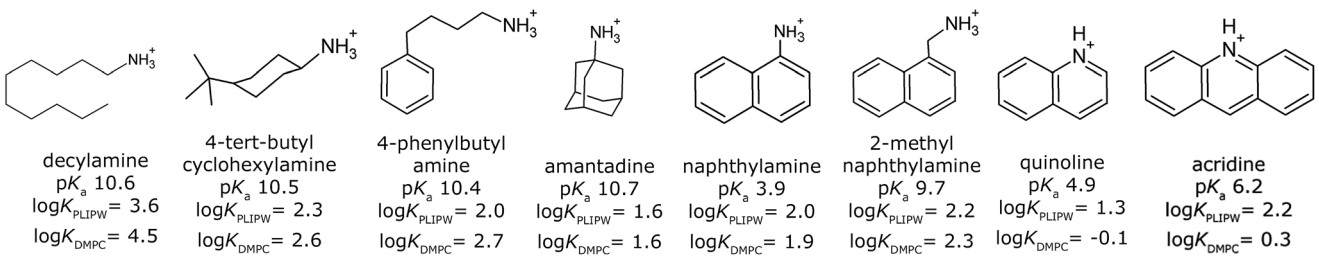

Fig. 5 Structures for $C_xH_yN^+$ amine series with 10 carbon atoms (first 5) and polyaromatic $C_xH_yN^+$ amines, along with dissociation constant (see Table S1†), measured membrane affinity (log K_{PLIPW} using IAM-HPLC) and simulated membrane affinity (log K_{DMPC} using COSMOmic).

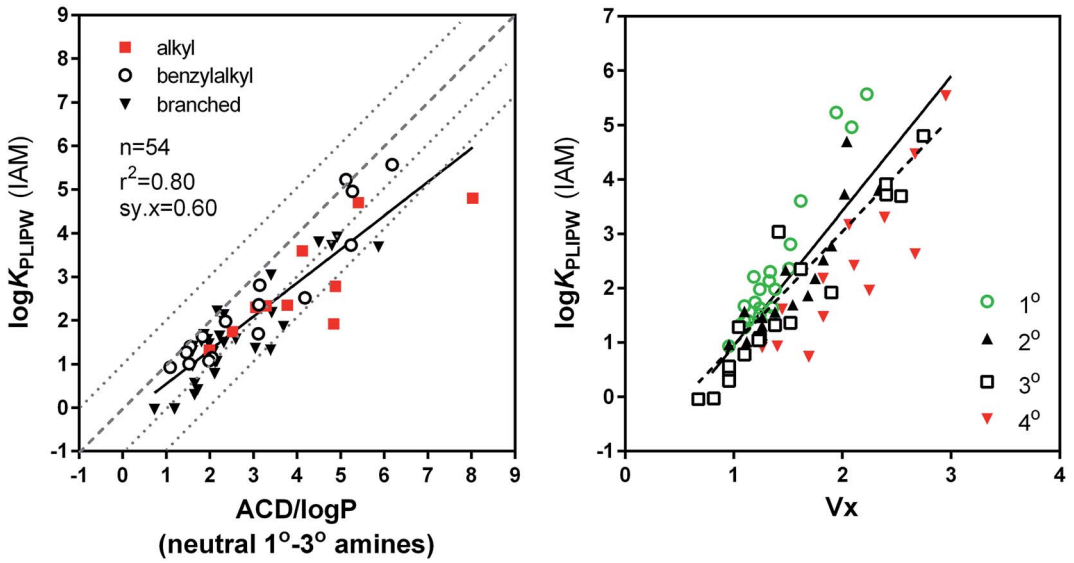

Fig. 6 Single parameter fitting of log *P* (using ACD labs values) and molecular volume (using McGowans Vx approach) for the membrane affinity of $C_xH_yN^+$ amines. Solid lines are the regressions in Table 2. Dotted and broken lines in the left graph indicate 0.1× − 1× − 10× and 100× differences between log *P* and log K_{PLIPW} values. The broken line in the right plot with Vx indicate the regression line if QACs (4°) are included.

ammonium compounds (QACs), McGowan's molecular volume Vx (Table 1) is also an equally suitable descriptor for $C_xH_yN^+$ amines (sy.x = 0.65 log units) as log *P* (Fig. 6 and Table 2). For the overall chemical domain of $C_xH_yN^+$ amines, a direct benefit of COSMOmic over log *P* would be the inclusion of quaternary ammonium structures and specific differences between structurally very different isomers. This is of interest for research on the membrane activity and cell toxicity of cationic salt species used in ionic liquids.[24] For the chemical domain of $C_xH_yN^+$ amines, the parameter Vx has the advantage of being a consistent, fast and free parameter while COSMOmic and ACD/Labs are commercial software packages. In addition, there are also other molecular simulation software packages and many different algorithms to calculate log *P* values that could confuse application of these regressions. Although Vx can be easily calculated for QACs, including the 14 QACs lowers the regression accuracy (sy.x = 0.76 log units, and R^2 = 0.68). For the chemical domain of all $C_xH_yN^+$ amines, the simple COSMOmic K_{DMPC} model (eqn (1), Table 2) differs more than threefold for 26%, and more than tenfold for 7% of the compounds, while the log *P* model (eqn (3), Table 2) differs more than threefold for 37%, and more than tenfold for 11% of the compounds. For low tier screening of the membrane affinity, these seem appropriately accurate.

3.5 Optimizing regressions with COSMOmic predicted K_{DMPC} for organic cations using a multiparameter approach

As discussed in Section 3.2, COSMOmic predictions on $C_xH_yN^+$ amines consistently deviate from IAM-HPLC data for the methyl groups on the charged nitrogen, excessively for polyaromatic *N*-heterocyclic compound acridine, and to a small extent for branched amines. Excepting acridine as a particular outlier (#42, see Fig. 5), we restrict the chemical domain to $C_xH_yN^+$ amines without polycyclic (>2) heteroaromatic compounds. Also, benzyltributylammonium (#66, B3BAm) significantly weakened the log K_{PLIPW}(IAM) *vs.* log K_{DMPC} (calc.) regression, as was also noted for sorption to natural organic matter and clay minerals.[19,22] We aimed to improve the simple log K_{PLIPW} − log K_{DMPC} model by accounting only for differences in amine type. Using multiple linear regression on the residuals (log K_{PLIPW} − log K_{DMPC}) of the current data set (so, without the outliers acridine and B3Bam, see ESI-Fig. S12†), we derived optimized corrective increments to log K_{DMPC} for different amine types (δ_{dmpc}): −0.51 for 1° amines, +0.34 for 2° amines, +0.76 for 3° amines, and +0.68 for 4° amines (see Table 2). According to these increment values, the δ-values compensate for overestimation of 1° amines by COSMOmic, and underestimation of 2° amines, 3° amines and QACs (ESI-Fig. S12†). These increments are not including the recommended offset value of −0.32 log units (average difference between observed and calculated log K_{lipw} values for both charged and neutral compounds) described in the study that optimized the membrane potential in COSMOmic calculations with the DMPC bilayer.[11] Fig. 7 shows that the predictive value of COSMOmic is considerably improved when only accounting for the amine type in this slightly narrower chemical applicability domain. With the additional δ parameters, the sy.x improved from 0.57 to 0.36 log units, and the compounds predicted within a factor of ±3 increased from 74% to 83%. With the exclusion of acridine and B3BAm, 99% of the compounds were predicted within a factor of ±10. In a similar manner to derivation of the δ_{dmpc} values, the amine type corrective increments for log *P* residuals ($\delta_{log\ P}$) are −0.35 for 1° amines, −1.03 for 2° amines, and −1.5 for 3° amines (Table 2). These values may be considered analogues to the Δmw values derived by other studies,[2,25] and are in the same range for these simple cationic structures. Including $\delta_{log\ P}$ in the log *P* model reduces the scatter compared

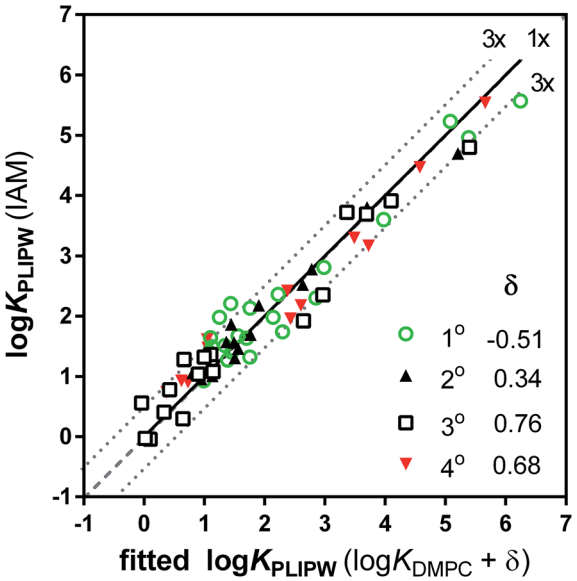

Fig. 7 IAM-HPLC based phospholipid sorption coefficients (log K_{PLIPW}) plotted against log K_{PLIPW} predictions for $C_xH_yN^+$ compounds, based on the 2-parameter relationship with the COSMOmic log K_{DMPC} value and amine type coefficient δ (eqn (2)). Broken line indicates 1 : 1 comparison, dotted lines a 3 : 1 difference, between observed and predicted values. Outliers acridine and benzyltributylammonium are left out.

to the single parameter log P regression (sy.x improved from 0.60 to 0.51), but the improvement is smaller compared to the log K_{DMPC} model eqn (1) and (2).

These "log K + δ" regressions (eqn (2) and (4) in Table 2) have the potential to improve chemical fate assessment studies in the chemical domain of $C_xH_yN^+$ amines. The $C_xH_yN^+$ chemical domain does not yet include cationic surfactants with alkylchains longer than C_{12}, which could not be determined experimentally by IAM-HPLC. Although COSMOmic input files are readily created, extrapolation to longer chains, especially with multiple longer chains, should be carried out with caution. The current data set includes the bioactive $C_xH_yN^+$ compounds amantadine, amphetamine, methamphetamine, tricyclic antidepressants (maprotiline, amitrityline and imipramine, for which the COSMOtherm structure suggests that the second N-atom is rendered nonpolar by the neighbouring phenyl rings), fenpropidin (fungicide), MPP^+ (neurotoxin and herbicide), individual benzalkonium homologues (biocides), alkylpyridinium (biocides). Obviously, the presence of polar groups in organic cations would render Vx useless as a single descriptor, necessitating many additional parameters to represent the additional polar interactions.[19,22] log P estimates and COSMOmic predictions should be able to include the polar interactions, potentially covering a much broader chemical domain of organic cations with 2 parameter regressions similar to those presented here.

Although the ability of COSMOmic to predict liposomal partitioning data for a variety of amine structures has been reported already,[11,15] the polar organic cations tested in the previous IAM-HPLC study of organic cations[15] provide a first evaluation using direct measurements with IAM-HPLC under optimized conditions (see Table S2†). Accounting for the δ_{dmpc} or $\delta_{log\ P}$ descriptors fitted with $C_xH_yN^+$ amines can be easily applied to other cationic compounds with polar groups. Fig. 8 plots the fitted phospholipid sorption coefficients for nine "polar" organic cations (tryptamine, amlodipine, metoprolol, atenolol, propranolol, fluoxetine, "dmapio", procaine and lidocaine) alongside the $C_xH_yN^+$ amines against IAM-HPLC data. Notably, the log P + δ regression (eqn (5)) tends to underpredict the sorption of these polar amines. The COSMOmic + δ_{dmpc} regression (eqn (3)) shows high predictive power for these polar amines too, similar to the $C_xH_yN^+$ amines. An evaluation on a much larger set of polar amines is needed to determine which types of organic cations appear to be problematic for COSMOmic, and which types of polar organic

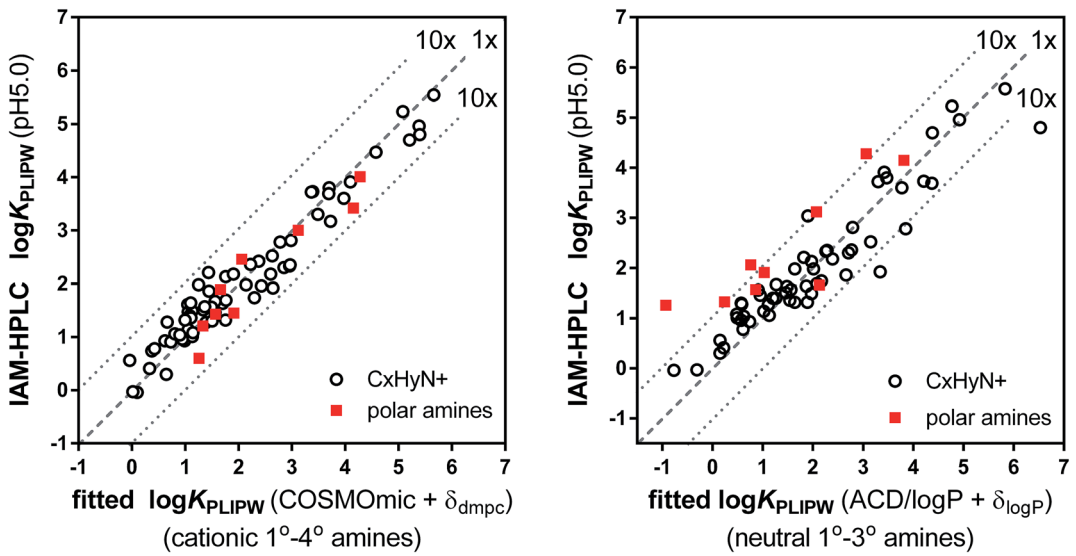

Fig. 8 IAM-HPLC based phospholipid sorption coefficients (log K_{PLIPW}) for polar organic cations from ref. 16 plotted against predictions from 2-parameter regressions with COSMOmic's log K_{DMPC} − δ and log P − δ.

cations can be readily included in the chemical domain of a quantum-chemistry based predictive model.

4. Conclusions

• Measurement of the retention time with the IAM-HPLC method appears to be an efficient way of deriving the sorption affinity into a phospholipid membrane (K_{PLIPW}) for a wide range of organic cation structures. These values could be used as direct input parameters for bioaccumulation models[2] and for interrogating the contribution of membrane partitioning in understanding toxicity pathways.

• The phospholipid-water distribution coefficient (D_{plipw}) at pH 7.4 is of highest relevance for (eco)toxicological modelling as this represents the physiological pH in most tissues. However, the IAM-HPLC method is hampered by (i) confounding electrostatic interactions between charged test compounds and the IAM-column material at eluent pH of 7.4,[15] and (ii) the operational range of IAM-HPLC being limited to pH 2.5–7.5. This particularly limits accurate D_{plipw} measurements for bases that are partly ionized at pH 7.4 ($pK_a \sim 6$–9), with unknown contributions of both neutral and ionic species to the overall D_{plipw}. For bases with $pK_a \geq 6$ IAM-HPLC measurements should be performed at sufficiently low pH to determine the membrane affinity of only the ionic species which will allow for a correct interpretation of IAM-HPLC measurements at pH 7.4. For bases with a $pK_a < 6$ IAM-HPLC can be used to measure the D_{plipw} at pH 7.4 directly without any confounding electrostatic effects.

• The differences in IAM-HPLC retention times between structurally different $C_xH_yN^+$ isomers, *e.g.* linear alkylamines *vs.* strongly branched amines with a comparable amount of carbon atoms, are consistent with advanced molecular simulations of the most favorable orientation and affinity of these sorbates in a fully hydrated phospholipid bilayer.

• The molecular features that extend into the hydrophobic bilayer domain for one compound, may be oriented most favorably in the polar headgroup domain of the bilayer for another compound. This strongly influences the contributions of any specific molecular feature to the overall K_{PLIPW}, hampering predictive approaches based on simple molecular fragments, or regressions with bulk solvent-water partition coefficients like log *P*.

• Molecular simulations of K_{PLIPW} with COSMOmic optimised for a DMPC bilayer appear to be so effective in dealing with the anisotropic membrane structure, that these computational predictions of the membrane affinity could be used in the absence of IAM-HPLC derived K_{PLIPW} values for wide ranges of molecules within the $C_xH_yN^+$ chemical domain, including quaternary ammonium compounds.

• Minor deviations between K_{PLIPW}(IAM) and K_{DMPC}-(COSMOmic) in the contribution of the amine type, or branching, and particularly N-heterocyclic structures, and of course more polar functionalities, should be studied in more detail in future research efforts. Validation of the IAM-HPLC data by additional measurements on key $C_xH_yN^+$ structures with dispersed single bilayer liposomes, or solid supported lipid membranes, would further strengthen this approach.

Acknowledgements

This study was funded by Unilever, Safety & Environmental Assurance Centre (SEAC), Colworth Science Park, United Kingdom.

References

1 A. Avdeef, *Absorption and Drug Development: Solubility, Permeability, and Charge State*, John Wiley & Sons, Inc., Hoboken, NJ, USA, 2003.
2 J. M. Armitage, J. A. Arnot, F. Wania and D. Mackay, *Environ. Toxicol. Chem.*, 2013, **32**, 115.
3 H. D. Bauerle and J. Seelig, *Biochem*, 1991, **30**, 7203.
4 D. Rhee, R. Markovich, W. G. Chae, X. Qiu and C. Pidgeon, *Anal. Chim. Acta*, 1994, **297**, 377.
5 C. Ottiger and H. Wunderli-Allenspach, *Pharm. Res.*, 1999, **16**, 643.
6 B. I. Escher, R. P. Schwarzenbach and J. C. Westall, *Environ. Sci. Technol.*, 2000, **34**, 3962.
7 A. Loidl-Stahlhofen, T. Hartmann, M. Schöttner, C. Rhöring, H. Brodowsky, J. Schmitt and J. Keldenich, *Pharm. Res.*, 2001, **18**, 1782.
8 B. I. Escher, R. I. L. Eggen, U. Schreiber, Z. Schreiber, E. Vye, B. Wisner and R. P. Schwarzenbach, *Environ. Sci. Technol.*, 2002, **36**, 1971.
9 A. Klamt, U. Huniar, S. Spycher and J. Keldenich, *J. Phys. Chem. B*, 2008, **112**, 12148.
10 S. Endo, B. I. Escher and K.-U. Goss, *Environ. Sci. Technol.*, 2011, **45**, 5912.
11 K. Bittermann, S. Spycher, S. Endo, L. Pohler, U. Huniar, K.-U. Goss and A. Klamt, *J. Phys. Chem. B*, 2014, **118**, 14833.
12 K.-U. Goss and R. P. Schwarzenbach, *Environ. Sci. Technol.*, 2001, **35**, 1–9.
13 M. H. Abraham, *J. Phys. Org. Chem.*, 1993, **6**, 660–684.
14 A. B. A. Boxall, M. A. Rudd, B. W. Brooks, *et al.*, *Environ. Health Perspect.*, 2012, **120**, 1221.
15 K. Bittermann, S. Spycher and K.-U. Goss, *Chemosphere*, 2016, **144**, 382.
16 S. T. J. Droge, *Anal. Chem.*, 2016, **88**, 960.
17 S. Ong and D. Pidgeon, *Anal. Chem.*, 1995, **67**, 2119.
18 S. Jakobtorweihen, T. Ingram and I. Smirnova, *J. Comput. Chem.*, 2013, **34**, 1332.
19 S. T. J. Droge and K.-U. Goss, *Environ. Sci. Technol.*, 2013, **47**, 798.
20 C. Hansch, D. Hoekman, A. Leo, L. Zhang and P. Li, *Toxicol. Lett.*, 1995, **79**, 45.
21 R. Fruttero, G. Caron, E. Fornatto, D. Boschi, G. Ermondi, A. Gasco, P. A. Carrupt and B. Testa, *Pharm. Res.*, 1998, **15**, 1407.
22 S. T. J. Droge and K.-U. Goss, *Environ. Sci. Technol.*, 2013, **47**, 14224.
23 R. P. Austin, A. M. Davis and C. N. Manners, *J. Pharm. Sci.*, 1995, **84**, 1180.
24 P. Galletti, D. Malferrari, C. Samorì, G. Sartor and E. Tagliavini, *Colloids Surf., B*, 2015, **125**, 142.
25 J. Neuwoehner, K. Fenner and B. I. Escher, *Environ. Sci. Technol.*, 2009, **43**, 6830.
26 J. M. Cabot, E. Fuguet and M. Rosés, *Electrophoresis*, 2014, **35**, 3564.